Lead Phosphate Particles in Tap Water: Challenges for Point-of-use Filters

Weiyi Pan[†], Elizabeth R. Johnson[†], and Daniel E. Giammar[*†]

[†]Department of Energy, Environmental & Chemical Engineering, Washington University in St. Louis, MO 63130, United States

***Corresponding Author**

Address: Campus Box 1180, One Brookings Drive, St. Louis, MO 63130

Phone: 314-935-6849; Fax: 314-935-7211

Email: giammar@wustl.edu

Table of Contents Graphic

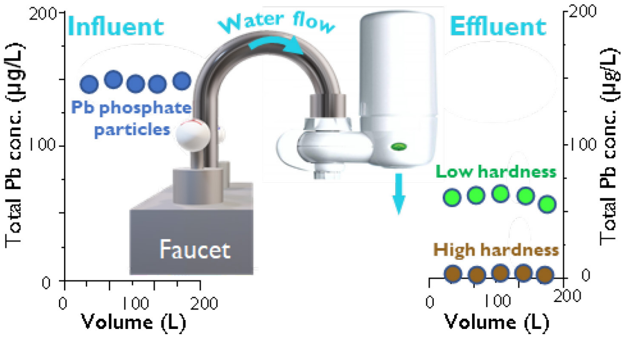

Abstract

To lower Pb concentrations in tap water, water systems implement corrosion control treatment that often involves the addition of orthophosphate. Because NSF/ANSI 53 (2018) certified point-of-use (POU) filters can remove Pb from tap water to <10 μg Pb/L, they are often distributed in emergencies or as follow-up steps to lead service line removals or disturbances. While these filters are certified for the removal of both soluble and particulate lead, this study reported that Pb phosphate particles can penetrate POU filters under certain conditions. The small sizes and negative surface charges of suspended Pb phosphate particles make them more mobile through the solid block activated carbon media of POU filters. When tested using challenging water containing 150 μg Pb/L, 2 mM ionic strength (IS), and no hardness at pH 7.0, 41% of the Pb passed through the POU filters. However, when IS was increased to 50 mM or Ca was increased to 0.5 mM, the amount of Pb penetrating the POU filters decreased to 32% and 17%, respectively. Adsorption of Ca onto Pb phosphate particles and high IS promotes aggregation and enhances POU filter performance.

Introduction

The main contributors of lead (Pb) in tap water are lead service lines (LSLs) and Pb-containing components of premise plumbing.[1–8] Although lead pipes were banned in potable water distribution systems in 1986 in the United States, millions of partial or whole LSLs are still in use.[9,10] The layers of lead corrosion products that form on the inner surface of LSLs play a crucial role in controlling dissolved Pb concentration and indirectly affect the formation of Pb-containing particles in tap water.[11] Dissolved Pb concentrations in tap water are controlled by the solubility of lead corrosion products, while particulate Pb concentrations are affected by the mobilization and deposition of these corrosion products.[12–17] Changes in water chemistry conditions can disturb the dissolution-precipitation equilibrium of pre-existing lead corrosion products and also induce the formation of Pb-containing particles in suspension in ways that increase Pb concentrations in the tap water.[18,19] For example, in Flint, MI, a change in water source and discontinuation of orthophosphate addition increased the solubility of lead corrosion products and mobilized both lead- and iron-containing particles.[20] Elevated Pb concentrations in tap water have also occurred after Newark, NJ decreased the pH of the tap water fed by their Pequannock Water Treatment Plant, and when University Park, IL changed their source water from well water to softened and filtered water from the Kankakee River.[21–23]

After elevated Pb concentrations are observed in tap water, a water system can follow several strategies to control Pb, including the addition of orthophosphate and replacement of LSLs.[18,24–26] Orthophosphate addition can lead to the formation of Pb phosphate solids, which have low solubilities and are beneficial for dissolved Pb control.[27,28] However, studies have reported that total Pb concentrations (dissolved and particulate lead) in tap water can remain high (> 50 μg/L) for months after phosphate addition.[29–31] A pipe loop study using high pH and low dissolved inorganic carbon (DIC) water conditions found that lead concentrations did not consistently drop below 15 μg/L until several months after orthophosphate addition had begun, while dissolved lead concentrations decreased almost immediately and stayed low.[24] A pipe loop study evaluating corrosion control treatment in the D.C. Water and Sewer Authority's distribution system found that it took six months of phosphate addition before lead concentrations consistently dropped below 15 μg/L.[32]

NSF/ANSI 53 certified point-of-use (POU) filters are distributed by some utilities in emergencies or after replacement or disturbance of a lead service line to mitigate the impact of high drinking water lead levels.[21] POU faucet filters typically contain solid block activated carbon (SBAC) and can remove both dissolved and particulate Pb. Granular activated carbon (GAC) is often used as filter media for POU pitcher filters. Both faucet and pitcher filters may have ion exchange in addition to SBAC or GAC to enhance their dissolved ion removal performance.[33] In Flint and Newark, POU faucet filters (with SBAC as filter media) were distributed to customers, and most of them effectively lowered the Pb concentration to the NSF/ANSI 53 certified value, which is 10 μg/L for NSF/ANSI 53 certification before 2019 and 5 μg/L for NSF/ANSI 53 certification after 2019.[34,35] However, they did not always perform as expected; five properly installed POU filters in Newark showed effluent lead concentrations of >10 μg/L.[35] A recent field study in Newark also observed Pb phosphate nanoparticles in the effluent from POU filters.[21]

The NSF/ANSI 53 certified POU filters may face underperformance under certain conditions.[21,35–37] Recently, a field investigation in Newark found that Pb phosphate nanoparticles (diameter <

0.1 μm) can penetrate properly installed and functional POU filters with total Pb concentrations in the filtered water as high as 45 μg/L.[21] Moreover, the NSF/ANSI 53 certification protocol challenges filters by using a $Pb(NO_3)_2$ solution to develop Pb carbonates and oxides that are 0.1-1.2 μm in size.[38] Well-dispersed Pb nanoparticles that are phosphate solids and not carbonates and oxides as well as particles with diameters smaller than 0.1 μm are therefore threats to POU filter performance.

Observations of POU filter underperformance in Newark were focused on this particular setting, and they pointed to a need to systematically evaluate the effect of Pb phosphate particles on POU filter performance under different aqueous conditions. These conditions (e.g. ionic strength (IS) and co-existing cations) play a crucial role in affecting Pb phosphate particle aggregation and, ultimately, may affect POU filter performance. Filters can remove particles from water mainly by two mechanisms: straining (when particles are larger than the void spaces in filter media) and contacting and attaching to the grains of the media (when particles are smaller than the voids).[39–41] Transport of particles to filter media surface occurs by sedimentation, diffusion, and interception, and attachment occurs by attractive close-range molecular forces such as hydrogen bonding and van der Waals forces.[41] The characteristics of different particles can affect their transport and attachment processes, which could lead to different POU filter performances.

The objective of this study was to determine the performance of POU filters for the removal of Pb phosphate nanoparticles over a range of relevant water chemistry conditions. The Pb phosphate nanoparticles were synthesized with different IS (2-50 mM as $NaNO_3$) and Ca concentrations (0-1.5 mM) and then characterized to understand their size, zeta potential, morphology, and crystallinity. The study yielded insights that can aid in the design of new POU filter media and the identification of potential revisions to the NSF/ANSI 53 certification protocol.

Materials and Methods

Materials

Commercially available NSF/ANSI 53 certified POU faucet filters (with SBAC as filter media, Figure S1) that are among the most widely used in the United States were purchased for use in this study. These filters received 2018 NSF/ANSI 53 certification, which requires that the maximum effluent concentration (MEC) of Pb is 10 μg/L.[26] Other chemicals and stock solutions are listed in the supporting information.

Pb phosphate nanoparticle stock solution preparation

Two sets of Pb phosphate nanoparticle solutions (Table 1) were synthesized with different IS (2, 10, 50 mM as $NaNO_3$) and Ca concentrations (0, 0.5, and 1.5 mM). The Pb/P mole ratio was 1:10. Detailed information about the selection of these conditions is delineated in the supporting information.

Table 1. Initial experimental conditions and zeta potentials of precipitates in Pb phosphate particle stock solutions

Set	**[a]Pb (μM)**	**[a]P (μM)**	**[b]Ca (mM)**	**[c]$NaNO_3$ (mM)**	**Zeta potential (mV)**

Control	7.25	72.5	/	2	−42.2 ± 2.6
IS = 10 mM	7.25	72.5	/	10	−39.1 ± 1.2
IS = 50 mM	7.25	72.5	/	50	−25.6 ± 0.7
Ca = 0.5 mM	7.25	72.5	0.5	2	−29.9 ± 1.4
Ca = 1.5 mM	7.25	72.5	1.5	2	−14.9 ± 0.8

[a]Pb and P: calculated total lead (added as $Pb(NO_3)_2$) and phosphate concentrations in the solutions. [b]Ca: calculated total calcium concentration, added as $Ca(NO_3)_2$. [c] $NaNO_3$: added to the solution to control the ionic strength.

POU filter performance test

All POU filters were flushed with reverse osmosis (RO) water to active them, and their abilities to remove dissolved lead were verified before their performance was tested with the waters containing suspended lead phosphate particles; details of these steps are in the supporting information. The experimental setup is shown in Figure S2. Each POU filter was then challenged with a total of 152 L (38 L per round for four rounds with the same challenge water condition) of Pb phosphate nanoparticle suspension (Pb_{total} = 150 µg/L) of a certain IS and Ca concentration. For each of the four rounds, two tanks were used. In each water condition, 40 L of suspension was prepared by mixing 4 L of Pb phosphate nanoparticle stock solution into 36 L of RO water with the same chemical conditions in a tank (pH, IS, and Ca concentrations, Table S1). The final solution was stirred for 5 min. The final total Pb concentrations in the tank were around 150 µg/L, and the total amounts of Pb in the tank matched that of the Pb phosphate nanoparticle stock solution. Transferring the Pb phosphate nanoparticle stock to the tank did not affect important particle characteristics (such as size); similar POU filter performance was observed when adding the premixed Pb phosphate nanoparticle stock to the tank as when the same amounts of $Pb(NO_3)_2$ and phosphate solutions were added directly to the tank (Figure S3). During each of the four rounds, 38 L (~10 gallons) of suspension were filtered through each POU filter. The remainder of the suspension was discarded. Between each round, the tanks and connecting pipes were flushed twice with 20 L of RO water to remove residual Pb(II). No Pb residual was detected after the cleaning. Because each filter only received a total of 190 L of water, the POU filters did not reach their designed treatment capacity (380 L). During each 38 L round, 0.5 L of influent was collected from the bottom valve of well-mixed tanks, and 1 L of effluent was collected in the middle of the run. Samples collected at different time points (at the beginning, middle, and end) during the run showed that effluent Pb concentrations remained consistent throughout the run (Figure S4). The performance test was modified from NSF/ANSI 53 with a shorter test time. All samples were digested with 2% nitric acid by volume for at least 16 hours in 1 L high-density polyethylene (HDPE) bottles before analysis of total lead by inductively coupled plasma mass spectrometry (ICP-MS, PerkinElmer, Ltd.) following EPA method 200.8.[42] All tests were conducted in duplicate and at room temperature (21 ± 1 °C).

Particle Characterization Methods

The formation and aggregation of Pb phosphate nanoparticles in the stock solutions were explored by monitoring their size evolution with DLS (Zetasizer, Malvern Instrument, Ltd.). The morphology and crystallinity of particles were observed by scanning electron microscopy (JEOL, Ltd.) and by transmission electron microscopy (TEM) with selected area electron diffraction (SAED) (JEOL, Ltd.). Detailed sample preparation and measurement protocols are listed in the supporting information.

Equilibrium Calculations

The pH, IS, and saturation indices (SI) of potential precipitates in the particle stock solutions were calculated using the MINTEQ database in Geochemist's Workbench (GWB, student version 14.0).[43] The calculations were conducted using the same conditions as the experiments. The solution was set to be in equilibrium with atmospheric CO_2.

Results and Discussion

Characterization of Pb phosphate nanoparticles

Based on GWB calculations (Table S2), all Pb phosphate particle stock solutions were supersaturated with respect to $Pb_5(PO_4)_3OH$ (hydroxylpyromorphite, SI = 12.4 ± 0.9) and $Pb_3(PO_4)_2$ (7.1 ± 0.5). After the stock solution was diluted in the tank, the SI values dropped to 4.4 ± 0.9 and 2.1 ± 0.6 for $Pb_5(PO_4)_3OH$ and $Pb_3(PO_4)_2$, respectively. In the presence of Ca, $Ca_5(PO_4)_3OH$ was also supersaturated in the Pb phosphate particle stock solution (SI = 5.4 ± 1.0) and the tank (SI = 2.4 ± 1.0). Under the initial solution conditions, hydroxylpyromorphite, which had the highest SI, would be expected to precipitate first. After the precipitation of hydroxylpyromorphite, soluble lead concentrations would drop to values that would leave the solution undersaturated with respect to the other solids. These calculations are consistent with lab-scale and field studies that observe hydroxylpyromorphite on the inner surfaces of lead pipes carrying water that is treated using orthophosphate.[30,31,44]

The SEM images (Figures 1a & 1b) show that all Pb phosphate particles had a similar sphere-like shape with a diameter smaller than 20 nm. With different IS (2-50 mM) and Ca concentrations (0-1.5 mM), no obvious size and morphology changes were observed (Figure S5). Similar morphology and size have been reported by Lytle et al. (2020), although the particles in that study were synthesized under different conditions (0.1 mg Pb/L, pH = 7.5, 7 mg C/L as DIC, and 3.4 mg PO_4/L).[45]

TEM results confirmed this particle size and provided information on the mineralogy, observing well-dispersed Pb phosphate nanoparticles with a diameter of 8.5 ± 3.6 nm (Figure 1c). The Pb phosphate nanoparticles synthesized in this experiment were smaller than those in some previous studies,[45,46] but close to the size range (10 – 200 nm) of Pb phosphate nanoparticles collected from POU filter effluent in Newark.[21] The SAED pattern identified the synthesized Pb phosphate nanoparticles as hydroxylpyromorphite. The electron diffraction pattern (Figure 1d) matched PDF No. 04-012-9459 (hydroxylpyromorphite), and detailed information is listed in Table S3. A similar SAED pattern of hydroxylpyromorphite has been observed in other studies.[21,47] This result was consistent with our calculations that suggested the precipitation of hydroxylpyromorphite. No Ca was added during the synthesis of these particles for SEM and TEM analyses, and the presence of Ca can result in Ca/Pb phosphate particle formation, which has a similar crystal structure as hydroxylpyromorphite.[18,48,49]

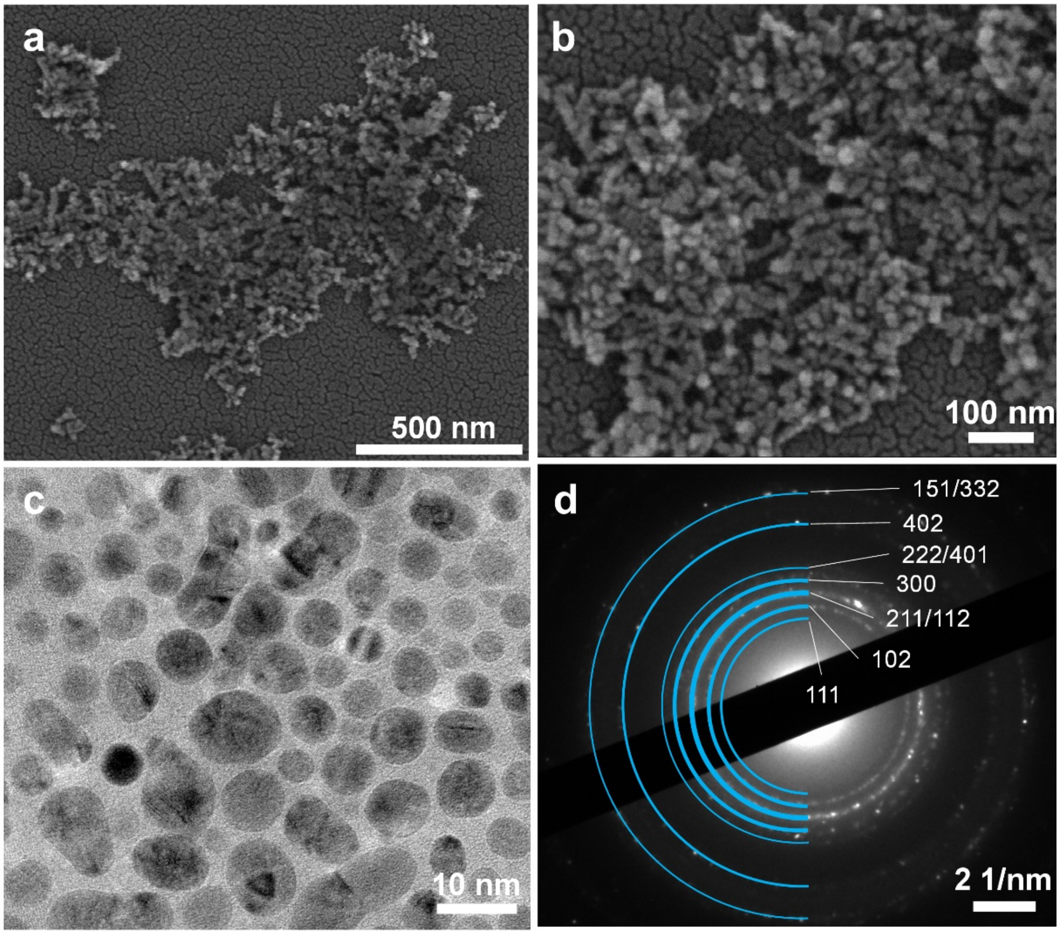

Figure 1. SEM images (a & b), TEM image (c), and selected area diffraction pattern (d) of Pb phosphate particles. The Pb phosphate particles were synthesized with a Pb/P ratio of 1/10 at pH 7. No Ca was present during the synthesis. The Miller indices (*hkl*) in the selected area diffraction pattern were determined based on the d-spacing of each ring and corresponding lattice spacing according to the hydroxylpyromorphite PDF card No. 04-012-9459.

Pb phosphate nanoparticle sizes and POU filter performance test

The size evolution of Pb phosphate particles formed in solutions with varied IS and Ca conditions are shown in Figures 2a and 2b. At IS = 2 mM, the D_H of the particles (63 ± 6 nm) remained unchanged within the 60 min duration of the DLS measurement. Lytle et al. (2020) also synthesized Pb phosphate nanoparticles under similar water chemistry conditions and reported a similar D_H (74 ± 11 nm).[45] 10 mM IS also did not affect the D_H, but 50 mM IS resulted in an increase in D_H to 400 nm over 1 h. With 0.5 mM and 1.5 mM Ca at IS = 2 mM, the D_H of Pb phosphate particles increased to ~ 420 nm and ~ 630 nm, respectively, over 1 h. These effects of IS and Ca were similar to the observations made by Zhao et al. (2018).[46]

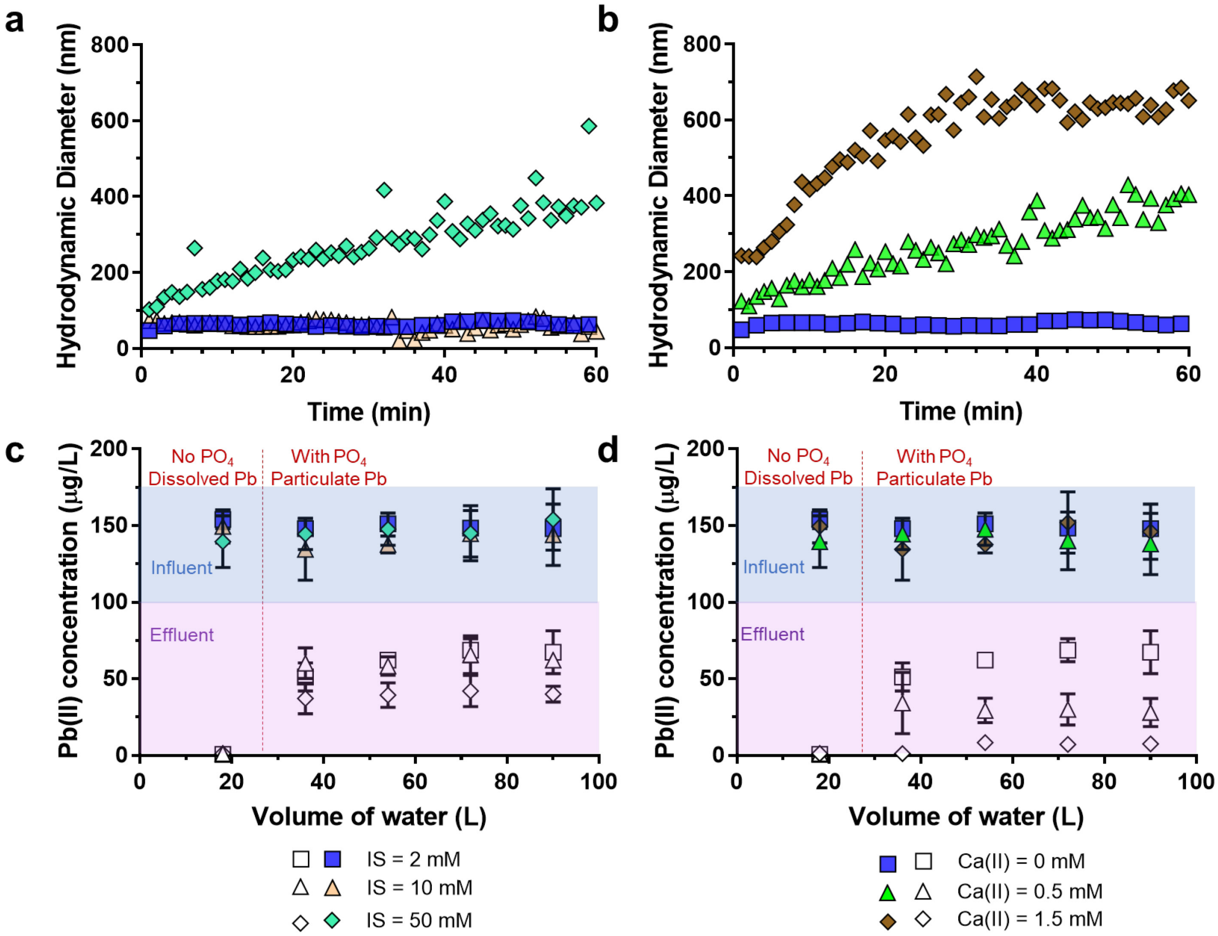

Figure 2. The hydrodynamic diameters of Pb phosphate particles formed at (a) different ionic strengths (controlled by 2-50 mM $NaNO_3$) and (b) different Ca concentrations (0-1.5 mM). The total Pb(II) concentrations in the influent/effluent during the POU filter performance test with (c) different IS (controlled by 2-50 mM $NaNO_3$) and (d) different Ca concentrations (0-1.5 mM) with 2 mM $NaNO_3$ to control the IS. The stages of each test with no PO_4 were used to confirm that the POU filters were functional when treating water with 150 µg/L of dissolved lead. All experiments were conducted at pH = 7.0 ± 0.1. Error bars represent the standard deviations from duplicate experiments.

POU filter performance was strongly related to the D_H of the Pb phosphate particles. The POU filter media has a porous structure (as shown in Figure S6) with a pore size range of 0.1-21 µm. When challenged by Pb phosphate particles, a larger D_H was associated with improved POU filter performance. At a D_H of 63 ± 6 nm (with IS = 2-10 mM, no Ca), 41% of Pb phosphate particles (~ 62 µg/L Pb) penetrated the POU filters and were detected in the filtered water (Figure 2c-d). However, at D_H ~ 400 nm (with IS = 50 mM or Ca = 0.5 mM), the total Pb concentration in the filtered water decreased to approximately 45 µg/L, and with a D_H of > 600 nm (with Ca = 1.5 mM), the total Pb concentration in filtered water met the effluent goal of NSF/ANSI 53 certification (< 10 µg/L). Higher IS yielded a larger D_H of Pb phosphate particles and therefore promoted POU filter performance, but ~39.4 µg/L Pb was still detected in the effluent even with IS = 50 mM. Because drinking water IS is typically lower than 11 mM, it is unlikely that IS would substantially affect POU filter performance under relevant conditions. With increasing Ca concentration, the

D_H of Pb phosphate particles increased, and the POU filter performance was promoted. The Ca concentration in tap water is related to hardness, which is the sum of the divalent cations (generally Ca^{2+} and Mg^{2+}).[50] High IS conditions resulted in lower absolute values of zeta potentials, and Ca^{2+} adsorption to negatively charged Pb phosphate particles can neutralize their surface charge. High IS and Ca therefore decreased repulsion both between particles and between the particles and the filter media, and hence they increased the proportion of Pb phosphate nanoparticles removed by POU filters.[50,51]

Extra considerations in POU filter use for lead removal may therefore be needed in water systems with low hardness (< 0.5 mM as Ca or 50 mg/L as $CaCO_3$) and use of phosphate as a corrosion inhibitor. For the Pequannock Gradient in Newark, the presence of LSLs, low hardness, and initiation of phosphate addition was almost optimal for the formation of stable Pb phosphate particles when underperformance of NSF/ANSI 53 certified POU filters was observed. [21,35] A recent field study confirmed the existence of Pb phosphate nanoparticles in the effluent of POU filters in Newark.[21]

The D_H values for Pb phosphate particles formed with IS = 50 mM and Ca = 0.5 mM were similar (383.4 and 403.7 nm), but the particles formed at IS = 10 mM had a more negative zeta potential (−39.1 ± 1.2, compared to −29.9 ± 1.4 mV). The POU filters removed a higher proportion of Pb phosphate particles with a less negative surface charge (−29.9 ± 1.4 mV). The filter media (SBAC) surface was negatively charged (as shown in Figure S7), which is similar to previous findings.[52] This surface charge information indicates that a less negative particle surface charge would be predicted to increase filter performance.

Environmental Implications

The performance of POU filters is dependent on the water chemistry. NSF/ANSI 53 certified POU filters cannot effectively remove Pb from all relevant tap water compositions. High IS (≥ 50 mM) and Ca concentrations (≥ 1.5 mM) promote aggregation of Pb phosphate particles and neutralize their surface charge, which leads to better POU filter performance. Other studies of Pb phosphate particle aggregation suggest that natural organic matter retards aggregation, which may cause POU filter underperformance, while different pH conditions in tap water (pH = 6 - 9) are unlikely to affect POU filter performance.[46]

The small size and negative surface charge of Pb phosphate nanoparticles create a new challenge for NSF/ANSI 53 certified POU filters. Although the latest NSF/ANSI 53 certification lowers the MEC to 5 μg/L, the challenge water for certification still consists of 0.1-1.2 μm Pb carbonate/hydroxide particles, so POU filter performance for removal of Pb phosphate nanoparticles remains unverified.[38] The surface charge and pore sizes of POU filter media can be improved to enhance its Pb phosphate particle removal performance. Changing the surface charge of POU filter media or portions of the media to less negatively or even positively charged would decrease the repulsive force between the media and Pb phosphate particles. Smaller pore sizes may be beneficial to increase Pb phosphate particle removal, but smaller pore sizes would likely also decrease the effluent flow rate. Besides, the NSF/ANSI 53 certification protocol could also be modified to include well-dispersed Pb phosphate nanoparticles to account for the increasingly widespread use of phosphate as a lead corrosion inhibitor.

Acknowledgments

This research was supported by the U.S. National Science Foundation (CHE 1709484). W.P. acknowledges fellowship support through the McDonnell International Scholars Academy at Washington University in St. Louis. This work was performed in part using the Nanoscale Research Facility at Washington University in St. Louis, a member of the National Nanotechnology Infrastructure Network (NNIN), which was supported by the National Science Foundation under Grant No. ECCS-0335765. We thank Anshuman Satpathy, Neha Sharma, Yao Ma, and Anushka Mishrra for assistance with experimental activities and helpful discussions.

Supporting Information

Supporting information is available free of charge on the ACS Publications website. The supporting information includes POU filter performance confirmation tests, procedures for DLS, SEM, and TEM, initial experimental conditions in the tanks, calculated saturation indices (SI), comparison of PDF and observed (electron diffraction) d-spacings, zeta potentials and hydrodynamic diameter of precipitates in Pb phosphate particle stock solutions, POU filter performance test experimental setups and results for comparison between adding Pb phosphate nanoparticle stock to the tank and adding the same amounts of Pb and phosphate solutions directly to the tanks, Pb concentrations in samples collected at different time points, SEM images of Pb phosphate particles synthesized under different condition, SEM images of the filter media, and zeta potential of the filter media.

References

(1) Del Toral, M. A.; Porter, A.; Schock, M. R. Detection and Evaluation of Elevated Lead Release from Service Lines: A Field Study. *Environ. Sci. Technol.* **2013**, *47*, 9300–9307.

(2) Commons, C. Effect of Partial Lead Service Line Replacement on Total Lead at the Tap in Cranston, Rhode Island. *J. New Engl. Water Work. Assoc.* **2012**, *126*, 128.

(3) Clark, B.; Masters, S.; Edwards, M. Profile Sampling to Characterize Particulate Lead Risks in Potable Water. *Environ. Sci. Technol.* **2014**, *48*, 6836–6843.

(4) Douglas, I.; Campbell, A.; Muylwyk, Q. Lead Control in Soft Water: Experience from a Canadian Utility. In *Proc. 2007 AWWA Ann. Conf., Toronto*; 2007.

(5) Deshommes, E.; Prévost, M.; Levallois, P.; Lemieux, F.; Nour, S. Application of Lead Monitoring Results to Predict 0–7 Year Old Children's Exposure at the Tap. *Water Res.* **2013**, *47*, 2409–2420.

(6) Cornwell, D.; Lytle, D. A. Lead and Copper Research. *J. Am. Water Works Assoc.* **2018**, *110*, 2–2.

(7) Edzwald, J. K.; Lytle, D. A. *Water Quality and Treatment A Handbook on Drinking Water*; McGrawHill, 2010.

(8) Deshommes, E.; Trueman, B.; Douglas, I.; Huggins, D.; Laroche, L.; Swertfeger, J.; Spielmacher, A.; Gagnon, G. A.; Prévost, M. Lead Levels at the Tap and Consumer Exposure from Legacy and Recent Lead Service Line Replacements in Six Utilities. *Environ. Sci. Technol.* **2018**, *52*, 9451–9459.

(9) Cornwell, D. A.; Brown, R. A.; Via, S. H. National Survey of Lead Service Line Occurrence. *J. Am. Water Works Assoc.* **2016**, *108*, 182–191.

(10) LaFrance, D. B. Open Channel -- Restoring Faith. *J. Am. Water Works Assoc.* **2016**, *108*, 10–10.

(11) Abokifa, A. A.; Biswas, P. Modeling Soluble and Particulate Lead Release into Drinking Water from Full and Partially Replaced Lead Service Lines. *Environ. Sci. Technol.* **2017**, *51*, 3318–3326.

(12) Xie, Y.; Wang, Y.; Singhal, V.; Giammar, D. E. Effects of PH and Carbonate Concentration on Dissolution Rates of the Lead Corrosion Product PbO_2. *Environ. Sci. Technol.* **2010**, *44*, 1093–1099.

(13) Xie, Y.; Wang, Y.; Giammar, D. E. Impact of Chlorine Disinfectants on Dissolution of the Lead Corrosion Product PbO_2. *Environ. Sci. Technol.* **2010**, *44*, 7082–7088.

(14) Noel, J. D.; Wang, Y.; Giammar, D. E. Effect of Water Chemistry on the Dissolution Rate Ofthe Lead Corrosion Product Hydrocerussite. *Water Res.* **2014**, *54*, 237–246.

(15) Wang, Y.; Jing, H.; Mehta, V.; Welter, G. J.; Giammar, D. E. Impact of Galvanic Corrosion on Lead Release from Aged Lead Service Lines. *Water Res.* **2012**, *46*, 5049–5060.

(16) Deshommes, E.; Laroche, L.; Nour, S.; Cartier, C.; Prévost, M. Source and Occurrence of

Particulate Lead in Tap Water. *Water Res.* **2010**, *44*, 3734–3744.

(17) Triantafyllidou, S.; Parks, J.; Edwards, M. Lead Particles in Potable Water. *J. Am. Water Works Assoc.* **2007**, *99*, 107–117.

(18) Bae, Y.; Pasteris, J. D.; Giammar, D. E. The Ability of Phosphate to Prevent Lead Release from Pipe Scale When Switching from Free Chlorine to Monochloramine. *Environ. Sci. Technol.* **2020**, *54*, 879–888.

(19) Pan, W.; Pan, C.; Bae, Y.; Giammar, D. Role of Manganese in Accelerating the Oxidation of Pb(II) Carbonate Solids to Pb(IV) Oxide at Drinking Water Conditions. *Environ. Sci. Technol.* **2019**, *53*, 6699–6707.

(20) Pieper, K. J.; Martin, R.; Tang, M.; Walters, L.; Parks, J.; Roy, S.; Devine, C.; Edwards, M. A. Evaluating Water Lead Levels during the Flint Water Crisis. *Environ. Sci. Technol.* **2018**, *52*, 8124–8132.

(21) Lytle, D. A.; Schock, M. R.; Formal, C.; Bennett-Stamper, C.; Harmon, S.; Nadagouda, M. N.; Williams, D.; Desantis, M. K.; Tully, J.; Pham, M. Lead Particle Size Fractionation and Identification in Newark, New Jersey's Drinking Water. *Environ. Sci. Technol.* **2020**, *54*, 13672–13679.

(22) US EPA. University Park Drinking Water https://www.epa.gov/il/university-park-drinking-water (accessed Oct 28, 2020).

(23) Sullivan, M.; Lopez, M. Compliance With Mandated Testing for Lead in Drinking Water in School Districts in New Jersey. *J. Environ. Health* **2019**, *82*, 14–19.

(24) Welter, G.; Schock, M. R.; Miller, S. A.; Razza, R.; Giammar, D. E. *Pipe Loop Studies of Orthophosphate Addition for Control of Lead Release in High pH , Low DIC Waters*; In *Proc. 2015 AWWA Ann. Conf., Slat Lake City*; 2015.

(25) Trueman, B. F.; Krkošek, W. H.; Gagnon, G. A. Effects of Ortho- and Polyphosphates on Lead Speciation in Drinking Water. *Environ. Sci. Water Res. Technol.* **2018**, *4*, 505–512.

(26) NSF International. NSF/ANSI 53-2018: Drinking Water Treatment Units - Health Effects. Ann Arbor, MI, 2018.

(27) Edwards, M.; McNeill, L. S. Effect of Phosphate Inhibitors on Lead Release from Pipes. *J. Am. Water Works Assoc.* **2002**, *94*, 79–90.

(28) McNeill, L. S.; Edwards, M. Phosphate Inhibitor Use at US Utilities. *J. Am. Water Works Assoc.* **2002**, *94*, 57–63.

(29) Churchill, D. M.; Mavinic, D. S.; Neden, D. G.; MacQuarrie, D. M. The Effect of Zinc Orthophosphate and PH-Alkalinity Adjustment on Metal Levels Leached into Drinking Water. *Can. J. Civ. Eng.* **2000**, *27*, 33–43.

(30) Miller, S. A. *Investigation of Lead Solubility and Orthophosphate Addition in High PH Low DIC Water*; Master Thesis, University of Cincinnati, 2014.

(31) Bae, Y.; Pasteris, J. D.; Giammar, D. E. Impact of Orthophosphate on Lead Release from Pipe Scale in High PH, Low Alkalinity Water. *Water Res.* **2020**, *177*, 115764.

(32) National Service Center for Environmental Publications; (NSCEP). *Review of the Interim Optimal Corrosion Control Treatment for Washington, D.C. Final Report*; 2007.

(33) Deshommes, E.; Zhang, Y.; Gendron, K.; Sauvé, S.; Edwards, M.; Nour, S.; Prévost, M. Lead Removal from Tap Water Using POU Devices. *J. Am. Water Works Assoc.* **2010**, *102*, 91–105.

(34) Bosscher, V.; Lytle, D. A.; Schock, M. R.; Porter, A.; Del Toral, M. POU Water Filters Effectively Reduce Lead in Drinking Water: A Demonstration Field Study in Flint, Michigan. *J. Environ. Sci. Heal. - Part A Toxic/Hazardous Subst. Environ. Eng.* **2019**, *54*, 484–493.

(35) CDM Smith. City of Newark Point-of-Use Filter Study (August-September 2019) Filter Results Report - Final. Newark, NJ, 2019.

(36) Purchase, J. M.; Rouillier, R.; Pieper, K. J.; Edwards, M. Understanding Failure Modes of NSF/ANSI 53 Lead-Certified Point-of-Use Pitcher and Faucet Filters. *Environ. Sci. Technol. Lett.* **2021**, *8*, 155–160.

(37) Ingber, S. Newark's Drinking Water Problem : Lead And Unreliable Filters. *NPR* **2019**, 10–13.

(38) NSF International. NSF/ANSI 53-2019: Drinking Water Treatment Units - Health Effects. Ann Arbor, MI, 2019.

(39) Crittenden, J. C.; Trussell, R. R.; Hand, D. W.; Howe, K. J.; Tchobanoglous, G. *MWH's Water Treatment*; John Wiley & Sons, Inc.: Hoboken, NJ, USA, 2012.

(40) Tufenkji, N.; Elimelech, M. Correlation Equation for Predicting Single-Collector Efficiency in Physicochemical Filtration in Saturated Porous Media. *Environ. Sci. Technol.* **2004**, *38*, 529–536.

(41) Howe, K. J.; Hand, D. W.; Crittenden, J. C.; Trussell, R. R.; Tchobanoglous, G. *Principles of Water Treatment*; John Wiley & Sons, 2012.

(42) U.S. EPA. Determination of Trace Elements in Waters and Wastes by Inductively Coupled Plasma - Mass Spectrometry. In *Methods for the Determination of Metals in Environmental Samples*; 1996; Vol. 4, pp 88–145.

(43) Gustaffson, J. P. Visual MINTEQ – a free equilibrium speciation model https://vminteq.lwr.kth.se/.

(44) Tully, J.; DeSantis, M. K.; Schock, M. R. Water Quality–Pipe Deposit Relationships in Midwestern Lead Pipes. *AWWA Water Sci.* **2019**, *1*, e1127.

(45) Lytle, D. A.; Formal, C.; Doré, E.; Muhlen, C.; Harmon, S.; Williams, D.; Triantafyllidou, S.; Pham, M. Synthesis and Characterization of Stable Lead(II) Orthophosphate Nanoparticle Suspensions. *J. Environ. Sci. Heal. Part A* **2020**, 1–9.

(46) Zhao, J.; Giammar, D. E.; Pasteris, J. D.; Dai, C.; Bae, Y.; Hu, Y. Formation and Aggregation of Lead Phosphate Particles: Implications for Lead Immobilization in Water Supply Systems. *Environ. Sci. Technol.* **2018**, *52*, 12612–12623.

(47) Cotter-Howells, J. D.; Champness, P. E.; Charnock, J. M. Mineralogy of Pb-P Grains in the Roots of Agrostis Capillaris L. by ATEM and EXAFS . *Mineral. Mag.* **1999**, *63*, 777–789.

(48) Schock, M. R.; Wagner, I.; Oliphant, R. J. The Corrosion and Solubility of Lead in Drinking Water. *Intern. Corros. water Distrib. Syst.* **1996**, *4*, 131–230.

(49) Hopwood, J. D.; Derrick, G. R.; Brown, D. R.; Newman, C. D.; Haley, J.; Kershaw, R.; Collinge, M. The Identification and Synthesis of Lead Apatite Minerals Formed in Lead Water Pipes. *J. Chem.* **2016**, *2016*.

(50) Patrick, L.; William, A. Water Chemistry: An Introduction to the Chemistry of Natural and Engineered Aquatic Sytems. Oxford University Press, USA 2011.

(51) Stumm, W.; Sigg, L.; Sulzberger, B. *Chemistry of the Solid-Water Interface : Processes at the Mineral-Water and Particle-Water Interface in Natural Systems*; Wiley, 1992.

(52) Lee, H. *Improving Activated Carbon Performance in Point Of Use and Municipal Processes*; Doctoral Dissertation, Arizona State University, 2018.